

The effect of substituents on the P-P and P=C bond properties in phosphanylphosphaalkenes

Aleksandra Ziółkowska, Wiktoria Błaszkiewicz, Tomasz Kruczyński

1. Experimental section	2
2. NMR spectra section	5
2.1. (<i>i</i> Pr ₂ N)PhPCl	5
2.2. (<i>i</i> Pr ₂ N)PhP-P(SiMe ₃) ₂ (1).....	6
2.3. (<i>i</i> Pr ₂ N)PhP-P(SiMe ₃)Li·3.3THF (2).....	9
2.4. Ph ₂ C=P-PPh(NiPr ₂) (3)	12
2.5. Reaction of Ph ₂ C=P-PPh(NiPr ₂) with <i>n</i> BuLi	15
2.6. Reaction of Ph ₂ C=P-PPh(NiPr ₂) with PhLi	17
3. X-ray section	18
3.1. Crystallographic data.....	19
3.2. Molecular structures	20
4. Theoretical Calculations	21
5. References	25

Key words: lithiated diphosphane, phosphanylophosphaalkene, carboanion, P-P bond

1. Experimental section

Materials and method

All synthetic procedures were performed under inert gas (Ar) and were carried out using mBraun glovebox and standard Schlenk techniques. All spectra in solution were recorded on Bruker AV400 MHz spectrometer (external standard tetramethylsilane for ^1H , ^{13}C ; 85% H_3PO_4 for ^{31}P). Elemental analysis for solid and liquid samples were recorded on Elementary Vario El Cube CHNS. $(i\text{Pr}_2\text{N})\text{PhPCl}$ and $\text{P}(\text{SiMe}_3)_2\text{Li}\cdot 2.0\text{THF}$, were prepared according to procedures in the literature.¹⁻³ Tetrahydrofuran (THF), dimethoxyethane (DME), pentane and toluene were dried over Na/K alloy. All solvents were distilled under argon atmosphere. Elemental analyses were recorded on Elementary Vario El Cube CHNS.

$(i\text{Pr}_2\text{N})\text{PhP-P}(\text{SiMe}_3)_2$ (1)

To a solution of $(i\text{Pr}_2\text{N})\text{PhPCl}$ (10.00 g, 0.0410 mol) in 10 mL of pentane in cooling bath (-50°C) a solution of $\text{P}(\text{SiMe}_3)_2\text{Li}\cdot 2.0\text{THF}$ (13.47 g; 0.0410 mol) in 20 mL of pentane was slowly transferred. A few minutes after mixing the substrates, the turbid mixture was removed from the bath stirred for about 1 h, after which the precipitate was filtered off. The filtrate was concentrated to 5 ml and placed at +4°C, where colorless crystals appeared after 24 hours. The resulting compound was isolated (13.05 g; 82%) and characterized as $(i\text{Pr}_2\text{N})\text{PhP-P}(\text{SiMe}_3)_2$.

Anal. Calcd for $\text{C}_{18}\text{H}_{37}\text{N}_1\text{P}_2\text{Si}_2$: C, 56.06; H, 9.67; N, 3.63%.

Found: C, 56.01; H, 9.64; N, 3.70%

^1H NMR (400 MHz, C_6D_6 , 298 K) δ: 7.84 (dt, 2H, $J_{\text{H-H}} = 7.2$ Hz, $J_{\text{P-H}} = 1.0$ Hz, $(i\text{Pr}_2\text{N})\text{PhP-P}(\text{SiMe}_3)_2$), 7.15 (dt, 2H, $J_{\text{H-H}} = 7.2$ Hz, $J_{\text{P-H}} = 1.9$ Hz, $(i\text{Pr}_2\text{N})\text{PhP-P}(\text{SiMe}_3)_2$), 7.04 (t, 1H, $J_{\text{H-H}} = 7.2$ Hz, $(i\text{Pr}_2\text{N})\text{PhP-P}(\text{SiMe}_3)_2$), 3.57 (broad m, 2H, $J_{\text{H-H}} = 6.8$ Hz, $(i\text{Pr}_2\text{N})\text{PhP-P}(\text{SiMe}_3)_2$), 1.31 (broad m, 2H, $J_{\text{H-H}} = 6.8$ Hz, $(i\text{Pr}_2\text{N})\text{PhP-P}(\text{SiMe}_3)_2$), 1.05 (broad m, 6H, $J_{\text{H-H}} = 6.8$ Hz, $(i\text{Pr}_2\text{N})\text{PhP-P}(\text{SiMe}_3)_2$), 0.22 (broad m, 6H, $J_{\text{P-H}} = 4.4$ Hz, $(i\text{Pr}_2\text{N})\text{PhP-P}(\text{SiMe}_3)_2$) ppm.

$^{31}\text{P}\{{}^1\text{H}\}$ NMR (162 MHz, C_6D_6 , 298 K) δ: 38.54 ($J_{\text{P-P}} = 271.8$ Hz, $(i\text{Pr}_2\text{N})\text{PhP-P}(\text{SiMe}_3)_2$), -175.97 ($J_{\text{P-P}} = 271.8$ Hz, $(i\text{Pr}_2\text{N})\text{PhP-P}(\text{SiMe}_3)_2$) ppm.

$^{13}\text{C}\{{}^1\text{H}\}$ NMR (100.6 MHz, C_6D_6 , 298 K) δ: 145.28 (dd, $J_{\text{P-C}} = 32.7$ Hz, $J_{\text{P-C}} = 3.6$ Hz, $(i\text{Pr}_2\text{N})\text{PhP-P}(\text{SiMe}_3)_2$), 132.45 (d, $J_{\text{P-C}} = 4.5$ Hz, $(i\text{Pr}_2\text{N})\text{PhP-P}(\text{SiMe}_3)_2$), 132.23 (d, $J_{\text{P-C}} = 3.6$ Hz, $(i\text{Pr}_2\text{N})\text{PhP-P}(\text{SiMe}_3)_2$), 128.63 (d, $J_{\text{P-C}} = 5.4$ Hz, $(i\text{Pr}_2\text{N})\text{PhP-P}(\text{SiMe}_3)_2$), 49.84 (broad s, $(i\text{Pr}_2\text{N})\text{PhP-P}(\text{SiMe}_3)_2$), 24.68 (d, $J_{\text{P-C}} = 5.4$ Hz, $(i\text{Pr}_2\text{N})\text{PhP-P}(\text{SiMe}_3)_2$), 24.02 (d, $J_{\text{P-C}} = 7.3$ Hz, $(i\text{Pr}_2\text{N})\text{PhP-P}(\text{SiMe}_3)_2$), 3.73 (dd, $J_{\text{P-C}} = 10.9$ Hz, $J_{\text{P-C}} = 3.6$ Hz, $(i\text{Pr}_2\text{N})\text{PhP-P}(\text{SiMe}_3)_2$) ppm.

$(i\text{Pr}_2\text{N})\text{PhP-P}(\text{SiMe}_3)\text{Li}\cdot 3\text{THF}$ (2)

A solution of $n\text{BuLi}$ (10.90 mL; 0.0272 mol; 2.5 M) was added dropwise to a solution of $(i\text{Pr}_2\text{N})\text{PhP-P}(\text{SiMe}_3)_2$ (10.00 g; 0.0259 mmol) in 20 mL of THF cooled to 0 °C. Immediately after mixing, the solution was warmed to room temperature and stirred for a further 24 h. Subsequently, the THF was removed under vacuum and the residue was dissolved in 20 mL of pentane and a few drops of THF. After 24 h at -23 °C, grew yellow crystals (10.24 g; 70%) characterized as $(i\text{Pr}_2\text{N})\text{PhP-P}(\text{SiMe}_3)\text{Li}\cdot 3\text{THF}$.

^1H NMR (400 MHz, C_6D_6 , 298 K) δ: 8.09 (t, 2H, $J_{\text{H-H}} = 7.0$ Hz, $(i\text{Pr}_2\text{N})\text{PhP-P}(\text{SiMe}_3)\text{Li}\cdot 3.3\text{THF}$), 7.16 (t, shielded by benzene signal 2H, $(i\text{Pr}_2\text{N})\text{PhP-P}(\text{SiMe}_3)\text{Li}\cdot 3.3\text{THF}$), 7.00 (t, 1H, $J_{\text{H-H}} = 7.6$ Hz, $(i\text{Pr}_2\text{N})\text{PhP-P}(\text{SiMe}_3)\text{Li}\cdot 3.3\text{THF}$), 3.70 (broad m, 2H, $J_{\text{H-H}} = 7.2$ Hz, $(i\text{Pr}_2\text{N})\text{PhP-P}(\text{SiMe}_3)\text{Li}\cdot 3.3\text{THF}$, methine group), 3.53 (quintet, 13.3 H, $J_{\text{H-H}} = 3.2$ Hz, $(\text{Cy}_2\text{N})\text{PhP-P}(\text{SiMe}_3)\text{Li}\cdot 3.3\text{THF}$), 1.49 (d, 6 H, $J_{\text{H-H}} = 6.6$ Hz, $(i\text{Pr}_2\text{N})\text{PhP-P}(\text{SiMe}_3)\text{Li}\cdot 3.3\text{THF}$, methul group), 1.36 (quintet, 13.3 H, $J_{\text{H-H}} = 7.2$ Hz, $(i\text{Pr}_2\text{N})\text{PhP-P}(\text{SiMe}_3)\text{Li}\cdot 3.3\text{THF}$), 1.28 (d, 6 H, $J_{\text{H-H}} = 6.6$ Hz, $(i\text{Pr}_2\text{N})\text{PhP-P}(\text{SiMe}_3)\text{Li}\cdot 3.3\text{THF}$, methyl group), 0.68 (d, 9H, $J_{\text{P-H}} = 3.4$ Hz, $(i\text{Pr}_2\text{N})\text{PhP-P}(\text{SiMe}_3)\text{Li}\cdot 3.3\text{THF}$) ppm.

$^{31}\text{P}\{\text{H}\}$ NMR (162 MHz, C₆D₆, 298 K) δ : 49.12 (d, $J_{\text{P-P}} = 289.1$ Hz, (*iPr*₂N)PhP-P(SiMe₃)Li·3.3THF), -200.03 (d, $J_{\text{P-P}} = 289.1$ Hz, (*iPr*₂N)PhP-P(SiMe₃)Li·3.3THF) ppm.

$^{13}\text{C}\{\text{H}\}$ NMR (100.6 MHz, C₆D₆, 298 K) δ : 131.47 (dd, $J_{\text{P-C}} = 19.1$ Hz, $J_{\text{P-C}} = 6.4$ Hz, (*iPr*₂N)PhP-P(SiMe₃)Li·3.3THF), 128.62 (s, shielded by benzene signal, (*iPr*₂N)PhP-P(SiMe₃)Li·3.3THF), 128.06 (d, $J_{\text{P-C}} = 4.54$ Hz, (*iPr*₂N)PhP-P(SiMe₃)Li·3.3THF), 125.84 (s, (*iPr*₂N)PhP-P(SiMe₃)Li·3.3THF), 68.72 (s, (*iPr*₂N)PhP-P(SiMe₃)Li·3.3THF), 48.79 (broad s, (*iPr*₂N)PhP-P(SiMe₃)Li·3.3THF, methine group), 26.00 (s, (*iPr*₂N)PhP-P(SiMe₃)Li·3.3THF), 25.04 (d, $J_{\text{P-C}} = 6.1$ Hz, (*iPr*₂N)PhP-P(SiMe₃)Li·3.3THF, methyl group), 24.70 (d, $J_{\text{P-C}} = 8.3$ ppm, (*iPr*₂N)PhP-P(SiMe₃)Li·3.3THF, methyl group), 6.26 (dd, $J_{\text{P-C}} = 10.0$ Hz, $J_{\text{P-C}} = 8.2$ Hz, (*iPr*₂N)PhP-P(SiMe₃)Li·3.3THF) ppm.

Ph₂C=P-PPh(N*iPr*₂) (3)

A solution of benzophenone (0.065 g; 3.588 mmol) in 5 mL of toluene was added to a solution of (*iPr*₂N)PhP-P(SiMe₃)Li·3.3THF (0.200 g; 3.588 mmol) in 5 mL of toluene. Immediately formed an intensely orange solution, which was stirred for about 15 min. After that the solvent was evaporated from the solution and 15 mL of pentane was added. The mixture was filtered and concentrated by $1/3$ volume. After 24 h at -23 °C orange powder (0.102 g; 70%) appeared and was characterized as Ph₂C=P-PPh(*iPr*₂N).

Anal. Calcd for C₂₅H₂₉N₁P₂: C, 74.06; H, 7.21; N, 3.45%.

Found: C, 74.00; H, 7.19; N, 3.48%

^1H NMR (400 MHz, Tol-d₈, 298 K) δ : 7.69 – 6.96 (15 H, Ph₂C=P-PPh(*iPr*₂) – aromatic protons), 3.36 (broad m, 2H, $J_{\text{H-H}} = 6.6$ Hz, Ph₂C=P-PPh(*iPr*₂) – methine group) 1.14 (d, 6H, $J_{\text{H-H}} = 6.6$ Hz, Ph₂C=P-PPh(*iPr*₂) methyl group), 0.94 (d, 6H, $J_{\text{H-H}} = 6.6$ Hz, Ph₂C=P-PPh(*iPr*₂) methyl group) ppm.

$^{31}\text{P}\{\text{H}\}$ NMR (162 MHz, Tol-d₈, 298 K) δ : 273.06 (d, $J_{\text{P-P}} = 248.9$ Hz, Ph₂C=P-PPh(*iPr*₂)), 50.31 (d, $J_{\text{P-P}} = 248.9$ Hz, Ph₂C=P-PPh(*iPr*₂)) ppm.

$^{13}\text{C}\{\text{H}\}$ NMR (100.6 MHz, Tol-d₈, 298 K) δ : 203.54 (dd, $J_{\text{P-C}} = 56.8$ Hz, $J_{\text{P-C}} = 20.4$ Hz, Ph₂C=P-PPh(*iPr*₂)), 146.06 (dd, $J_{\text{P-C}} = 56.8$ Hz, $J_{\text{P-C}} = 20.4$ Hz, Ph₂C=P-PPh(*iPr*₂)), 144.90 (dd, $J_{\text{P-C}} = 13.6$ Hz, $J_{\text{P-C}} = 8.2$ Hz, Ph₂C=P-PPh(*iPr*₂)), 142.06 dd, $J_{\text{P-C}} = 23.6$ Hz, $J_{\text{P-C}} = 9.9$ Hz, Ph₂C=P-PPh(*iPr*₂)), 137.75 (s, Ph₂C=P-PPh(*iPr*₂)), 137.40 (s, Ph₂C=P-PPh(*iPr*₂)), 131.87 (s, Ph₂C=P-PPh(*iPr*₂)), 131.32 (dd, $J_{\text{P-C}} = 17.3$ Hz, $J_{\text{P-C}} = 4.5$ Hz, Ph₂C=P-PPh(*iPr*₂)), 129.95 (s, Ph₂C=P-PPh(*iPr*₂)), 129.04 (dd, $J_{\text{P-C}} = 18.2$ Hz, $J_{\text{P-C}} = 4.5$ Hz, Ph₂C=P-PPh(*iPr*₂)), 128.97 (d, $J_{\text{P-C}} = 10.9$ Hz, Ph₂C=P-PPh(*iPr*₂)), 128.03 (s, Ph₂C=P-PPh(*iPr*₂)), 127.97 (d, $J_{\text{P-C}} = 2.72$ Hz, Ph₂C=P-PPh(*iPr*₂)), 127.62 (dd, $J_{\text{P-C}} = 11.8$ Hz, $J_{\text{P-C}} = 6.4$ Hz, Ph₂C=P-PPh(*iPr*₂)), 127.55 (s, Ph₂C=P-PPh(*iPr*₂)), 125.26 (s, Ph₂C=P-PPh(*iPr*₂)), 49.42 (d, $J_{\text{P-C}} = 9.0$ Hz, Ph₂C=P-PPh(*iPr*₂) – methine group), 25.25 (d, $J_{\text{P-C}} = 2.7$ Hz, Ph₂C=P-PPh(*iPr*₂) – methyl group), 25.16 ppm, d, $J_{\text{P-C}} = 1.8$ Hz, Ph₂C=P-PPh(*iPr*₂) – methyl group) ppm.

[(*iPr*₂N)PhP-P(*nBu*)-CPh₂]⁻[Li(DME)₃]⁺ (3a)

To a solution of Ph₂C=P-PPh(*iPr*₂) (0.100 g; 0.247 mmol) in 5 mL of THF, cooled to -20 °C a solution of *nBu*Li (0.100 mL; 0.247 mmol; 2.5 M) was slowly added. The solution immediately turned amaranth in color. After about 10 min it was allowed to reach ambient temperature. In the next step, THF was evaporated and 3 mL of DME and a few drops of pentane was added. After 24 h at -23 °C red crystals appeared (0.092 g; 50%) which were characterized as [(*iPr*₂N)PhP-P(*nBu*)-CPh₂]⁻[Li(DME)₃]⁺.

Anal. Calcd for C₄₁H₆₈NP₂LiO₆: C, 66.56; H, 9.26; N, 1.89%.

Found: C, 66.75 H, 9.43; N, 2.05%

^1H NMR (400 MHz, Tol-d₈, 298 K) δ : 7.64 ppm – 6.88 (15 H, [(*iPr*₂N)PhP-P(*nBu*)-CPh₂]⁻[Li(DME)₃]⁺ - aromatic protons), 3.46 (s, 12H, [(*iPr*₂N)PhP-P(*nBu*)-CPh₂]⁻[Li(DME)₃]⁺ - methylene protons), 3.31 (s,

15H, $[(iPr_2N)PhP-P(nBu)-CPh_2]^-[Li(DME)_3]^+$ – methyl protons), 1.25 ppm – 1.19 (broad m, 2H $[(iPr_2N)PhP-P(nBu)-CPh_2]^-[Li(DME)_3]^+$ – methylene protons), 1.16 (d, 6H, $J_{H-H} = 6.6$ Hz, $[(iPr_2N)PhP-P(nBu)-CPh_2]^-[Li(DME)_3]^+$ – methyl protons), 0.98 (q, 6H, $J_{H-H} = 6.8$ Hz, $[(iPr_2N)PhP-P(nBu)-CPh_2]^-[Li(DME)_3]^+$ – methyl protons), 0.90 (broad d, $J_{H-H} = 6.7$, $[(iPr_2N)PhP-P(nBu)-CPh_2]^-[Li(DME)_3]^+$ - methylene protons), 0.76 (broad t, $J_{H-H} = 6.7$ Hz, $[(iPr_2N)PhP-P(nBu)-CPh_2]^-[Li(DME)_3]^+$ – methyl protons) ppm.

$^{31}P\{^1H\}$ NMR (162 MHz, Tol-d₈, 298 K) δ: 42.99 (d, $J_{P-P} = 192.5$ Hz, $[(iPr_2N)PhP-P(nBu)-CPh_2]^-[Li(DME)_3]^+$), 42.91 (d, $J_{P-P} = 192.9$ Hz, $[(iPr_2N)PhP-P(nBu)-CPh_2]^-[Li(DME)_3]^+$), 40.03 (d, $J_{P-P} = 207.9$ Hz, $[(iPr_2N)PhP-P(nBu)-CPh_2]^-[Li(DME)_3]^+$), 39.93 (d, $J_{P-P} = 208.2$ Hz, $[(iPr_2N)PhP-P(nBu)-CPh_2]^-[Li(DME)_3]^+$), -26.66 (d, $J_{P-P} = 208.2$ Hz, $[(iPr_2N)PhP-P(nBu)-CPh_2]^-[Li(DME)_3]^+$), -26.31 (d, $J_{P-P} = 207.9$ Hz, $[(iPr_2N)PhP-P(nBu)-CPh_2]^-[Li(DME)_3]^+$), -31.07 (d, $J_{P-P} = 192.9$ Hz, $[(iPr_2N)PhP-P(nBu)-CPh_2]^-[Li(DME)_3]^+$), -30.76 (d, $J_{P-P} = 192.5$ Hz, $[(iPr_2N)PhP-P(nBu)-CPh_2]^-[Li(DME)_3]^+$) ppm.

$^{13}C\{^1H\}$ NMR (100.6 MHz, Tol-d₈, 298 K) δ: 142.87 (d, $J_{P-C} = 4.5$ Hz, $[(iPr_2N)PhP-P(nBu)-CPh_2]^-[Li(DME)_3]^+$), 142.37 (d, $J_{P-C} = 13.6$ Hz, $[(iPr_2N)PhP-P(nBu)-CPh_2]^-[Li(DME)_3]^+$), 132.85 (dd, $J_{P-C} = 21.8$ Hz, $J_{P-C} = 8.2$ Hz, $[(iPr_2N)PhP-P(nBu)-CPh_2]^-[Li(DME)_3]^+$), 131.19 (dd, $J_{P-C} = 22.7$ Hz, $J_{P-C} = 5.4$ Hz, $[(iPr_2N)PhP-P(nBu)-CPh_2]^-[Li(DME)_3]^+$), 129.94 (d, $J_{P-C} = 11.8$ Hz, $[(iPr_2N)PhP-P(nBu)-CPh_2]^-[Li(DME)_3]^+$), 129.00 (d, $J_{P-C} = 9.1$ Hz, $[(iPr_2N)PhP-P(nBu)-CPh_2]^-[Li(DME)_3]^+$), 128.65 (d, $J_{P-C} = 5.4$ Hz, $[(iPr_2N)PhP-P(nBu)-CPh_2]^-[Li(DME)_3]^+$), 128.42 (broad, m, $[(iPr_2N)PhP-P(nBu)-CPh_2]^-[Li(DME)_3]^+$), 127.95 (s, $[(iPr_2N)PhP-P(nBu)-CPh_2]^-[Li(DME)_3]^+$), 127.81 (s, $[(iPr_2N)PhP-P(nBu)-CPh_2]^-[Li(DME)_3]^+$), 127.75 (s, $[(iPr_2N)PhP-P(nBu)-CPh_2]^-[Li(DME)_3]^+$), 127.48 (s, $[(iPr_2N)PhP-P(nBu)-CPh_2]^-[Li(DME)_3]^+$), 127.40 (d, $J_{P-C} = 6.3$ Hz, $[(iPr_2N)PhP-P(nBu)-CPh_2]^-[Li(DME)_3]^+$), 125.89 (s, $[(iPr_2N)PhP-P(nBu)-CPh_2]^-[Li(DME)_3]^+$), 125.72 (d, $J_{P-C} = 12.7$ Hz, $[(iPr_2N)PhP-P(nBu)-CPh_2]^-[Li(DME)_3]^+$), 71.78 (s, $[(iPr_2N)PhP-P(nBu)-CPh_2]^-[Li(DME)_3]^+$), 57.92 (s, $[(iPr_2N)PhP-P(nBu)-CPh_2]^-[Li(DME)_3]^+$), 49.07 (broad s, $[(iPr_2N)PhP-P(nBu)-CPh_2]^-[Li(DME)_3]^+$), 30.11 (dd, $J_{P-C} = 17.2$ Hz, $J_{P-C} = 9.1$ Hz, $[(iPr_2N)PhP-P(nBu)-CPh_2]^-[Li(DME)_3]^+$), 29.71 (d, $J_{P-C} = 5.2$ Hz, $[(iPr_2N)PhP-P(nBu)-CPh_2]^-[Li(DME)_3]^+$), 29.52 (d, $J_{P-C} = 5.1$ Hz, $[(iPr_2N)PhP-P(nBu)-CPh_2]^-[Li(DME)_3]^+$), 23.51 (d, $J_{P-C} = 5.28$ Hz, $[(iPr_2N)PhP-P(nBu)-CPh_2]^-[Li(DME)_3]^+$), 23.07 (d, $J_{P-C} = 6.4$ Hz, $[(iPr_2N)PhP-P(nBu)-CPh_2]^-[Li(DME)_3]^+$), 13.02 (s, $[(iPr_2N)PhP-P(nBu)-CPh_2]^-[Li(DME)_3]^+$) ppm.

Ph₂C(Li)-P(Ph)-PPh(NiPr₂) (3b)

To a solution of Ph₂C=P-PPh(NiPr₂) (0.100 g; 0.247 mmol) in 2 mL of THF-d₈, cooled to -10 °C a solution of PhLi (0.130 mL; 0.247 mmol; 1.9 M) was slowly added. The solution immediately turned dark red. After about 10 min it was allowed to reach ambient temperature and $^{31}P\{^1H\}$ NMR spectrum was measured. Formed compound was characterized as Ph₂C(Li)=P(nBu)-PPh(NiPr₂) (**3b**).

$^{31}P\{^1H\}$ NMR (162 MHz, Tol-d₈, 298 K) δ: 49.15 (d, $J_{P-P} = 152.8$ Hz, $[(iPr_2N)PhP-P(Ph)-CPh_2]Li$), 41.18 (d, $J_{P-P} = 186.5$ Hz, $[(iPr_2N)PhP-P(Ph)-CPh_2]Li$), -17.76 (d, $J_{P-P} = 186.4$ Hz, $[(iPr_2N)PhP-P(Ph)-CPh_2]Li$), -24.99 (d, $J_{P-P} = 152.8$ Hz, $[(iPr_2N)PhP-P(Ph)-CPh_2]Li$) ppm.

2. NMR spectra section

2.1. (*i*Pr₂N)PhPCl

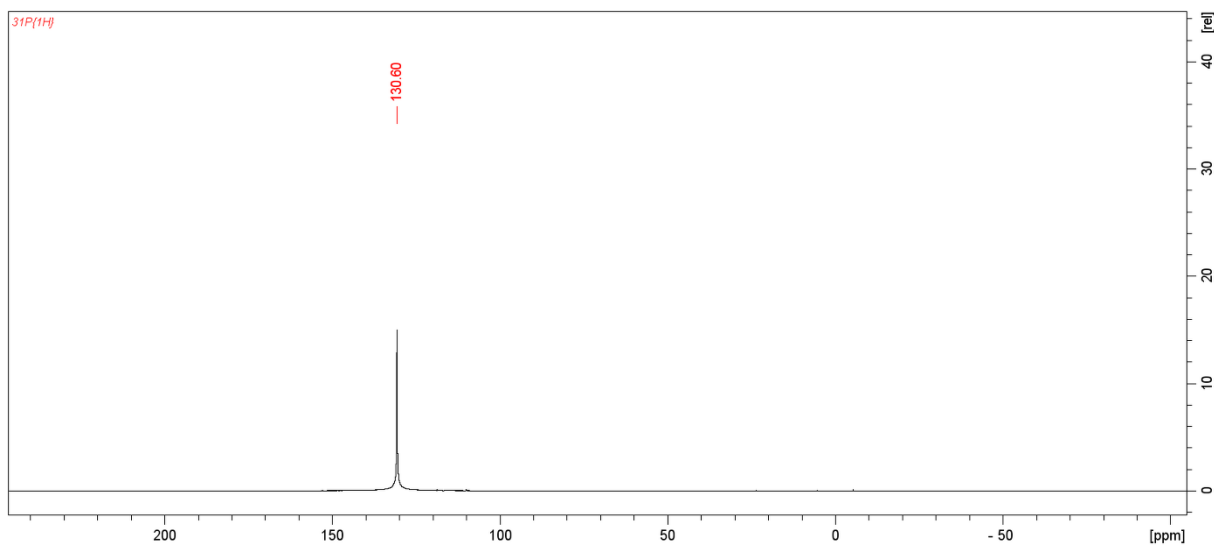


Figure S1. ³¹P{¹H} NMR (162 MHz, C₆D₆, 298 K) spectrum of isolated (iPr₂N)PhPCl.

130.60 ppm, s, (iPr₂N)PhPCl.

2.2. (*i*Pr₂N)PhP-P(SiMe₃)₂ (1)

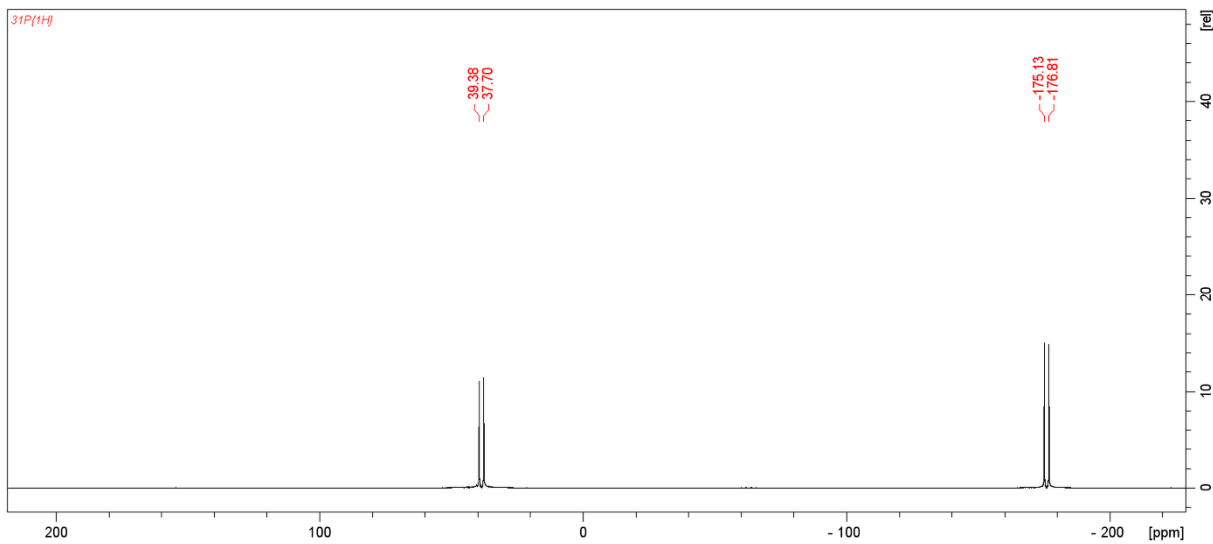


Figure S2. $^{31}\text{P}\{^1\text{H}\}$ NMR (162 MHz, C_6D_6 , 298 K) spectrum of isolated ($i\text{Pr}_2\text{N}$)PhP-P(SiMe₃)₂.

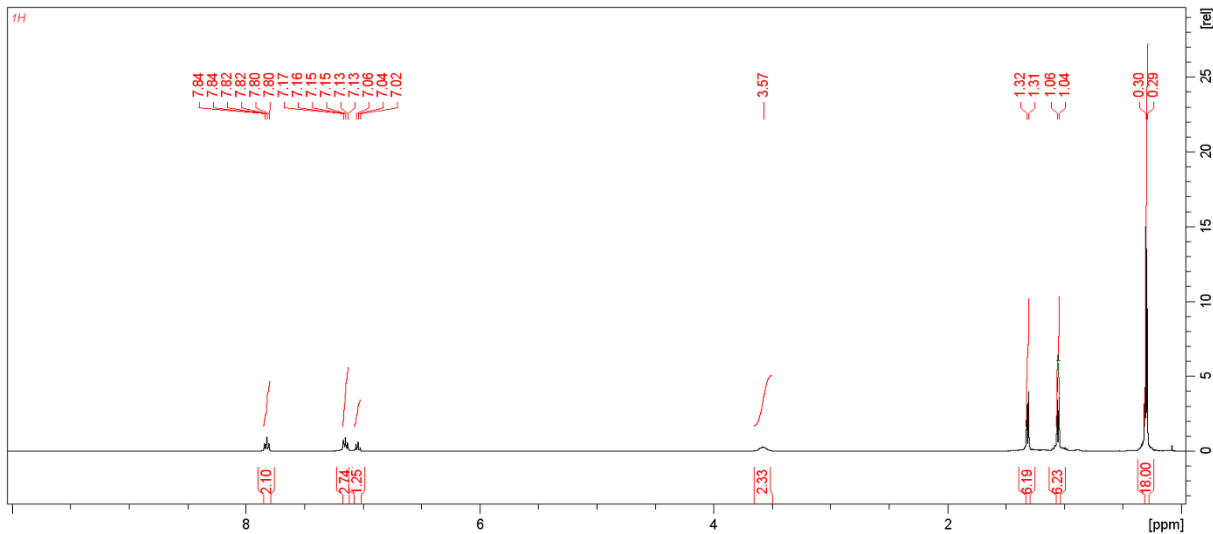


Figure S3. ^1H NMR (400 MHz, C_6D_6 , 298 K) spectrum of isolated (*i*Pr₂N)PhP-P(SiMe₃)₂.

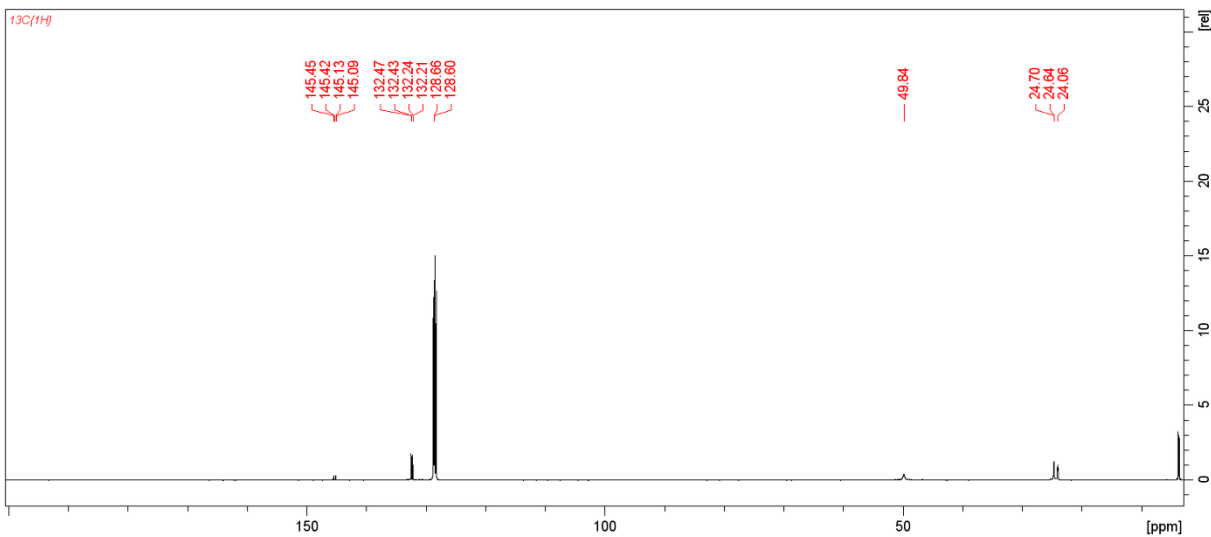


Figure S4. $^{13}\text{C}\{^1\text{H}\}$ NMR (100.6 MHz, C_6D_6 , 298 K) spectrum of isolated $(i\text{Pr}_2\text{N})\text{PhP-P}(\text{SiMe}_3)_2$.

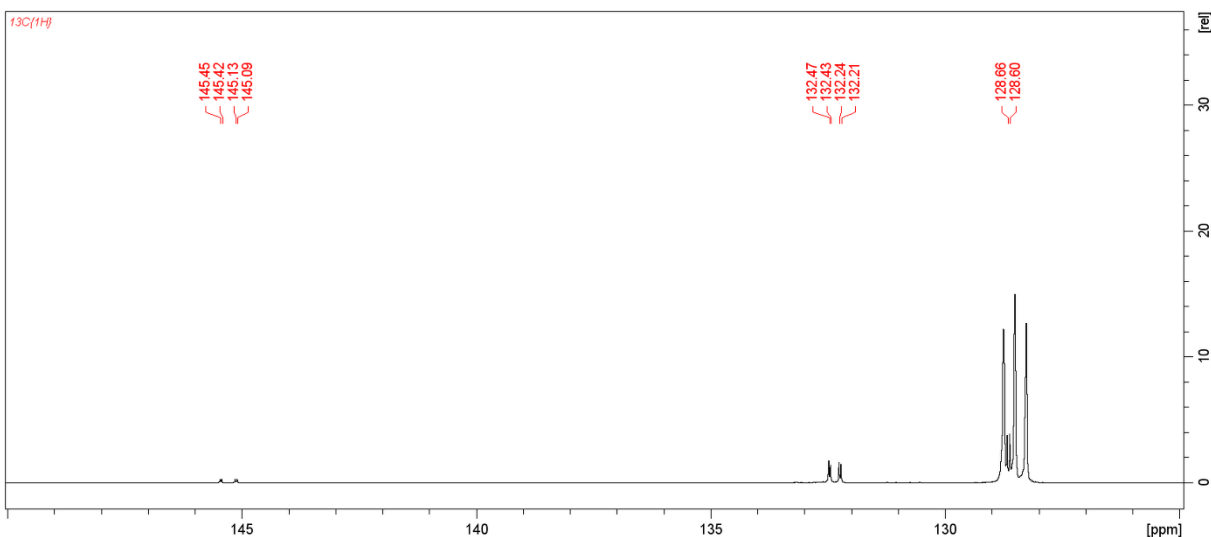


Figure S5. $^{13}\text{C}\{^1\text{H}\}$ NMR (100.6 MHz, C_6D_6 , 298 K) spectrum of isolated $(i\text{Pr}_2\text{N})\text{PhP-P}(\text{SiMe}_3)_2$ in the narrow range from 145 ppm to 125 ppm.

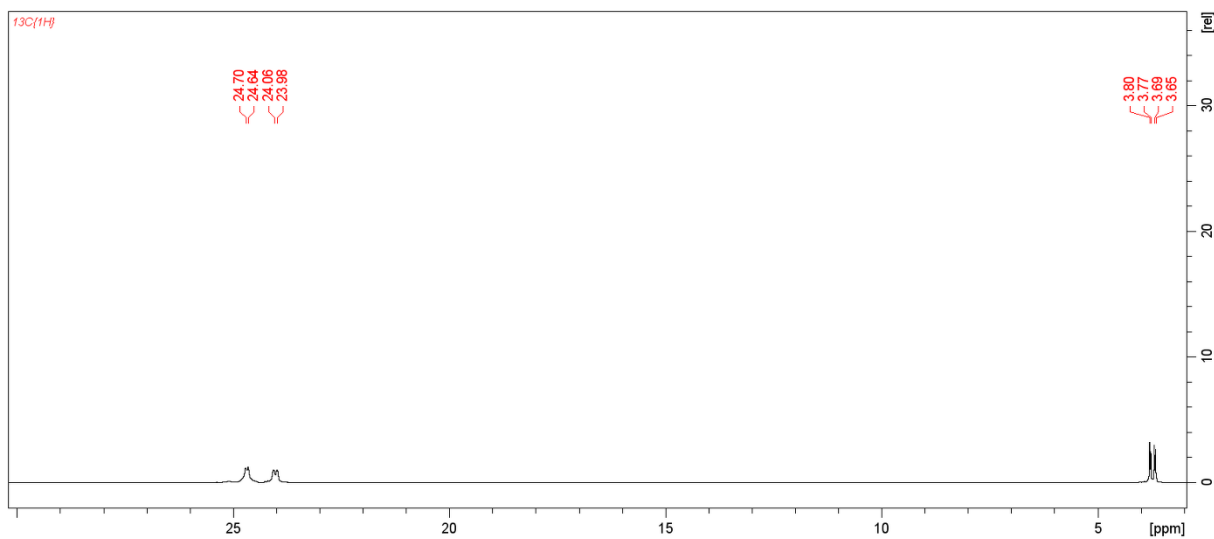


Figure S6. $^{13}\text{C}\{^1\text{H}\}$ NMR (100.6 MHz, C_6D_6 , 298 K) spectrum of isolated $(i\text{Pr}_2\text{N})\text{PhP-P}(\text{SiMe}_3)_2$ in the narrow range from 25 ppm to 0 ppm.

2.3. (*i*Pr₂N)PhP-P(SiMe₃)Li·3.3THF (2)

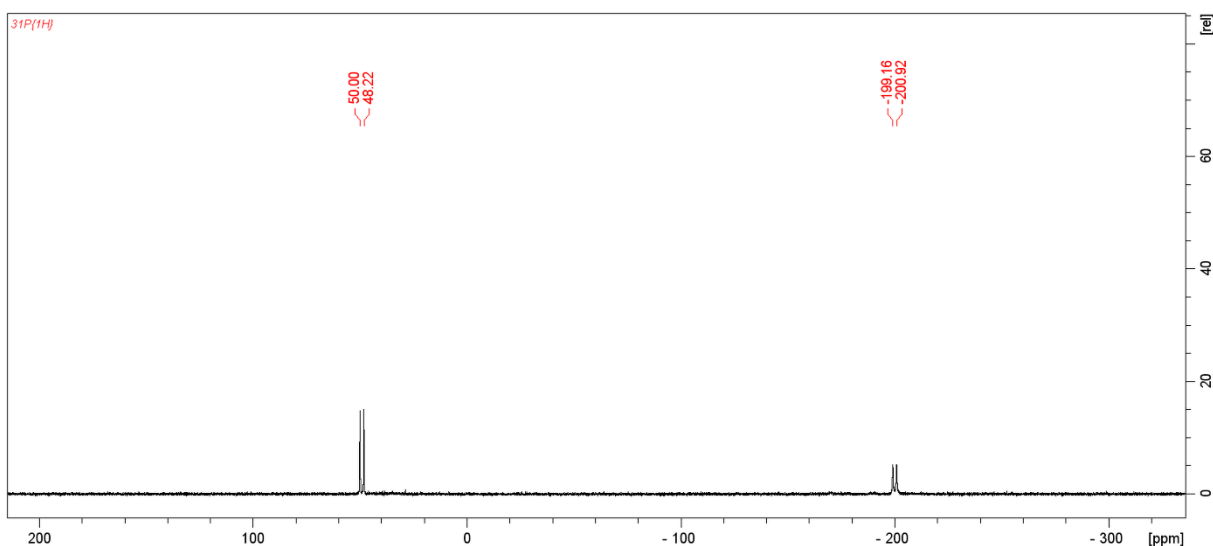


Figure S7. ³¹P{¹H} NMR (162 MHz, C₆D₆, 298 K) spectrum of isolated (*i*Pr₂N)PhP-P(SiMe₃)Li·3.3THF.

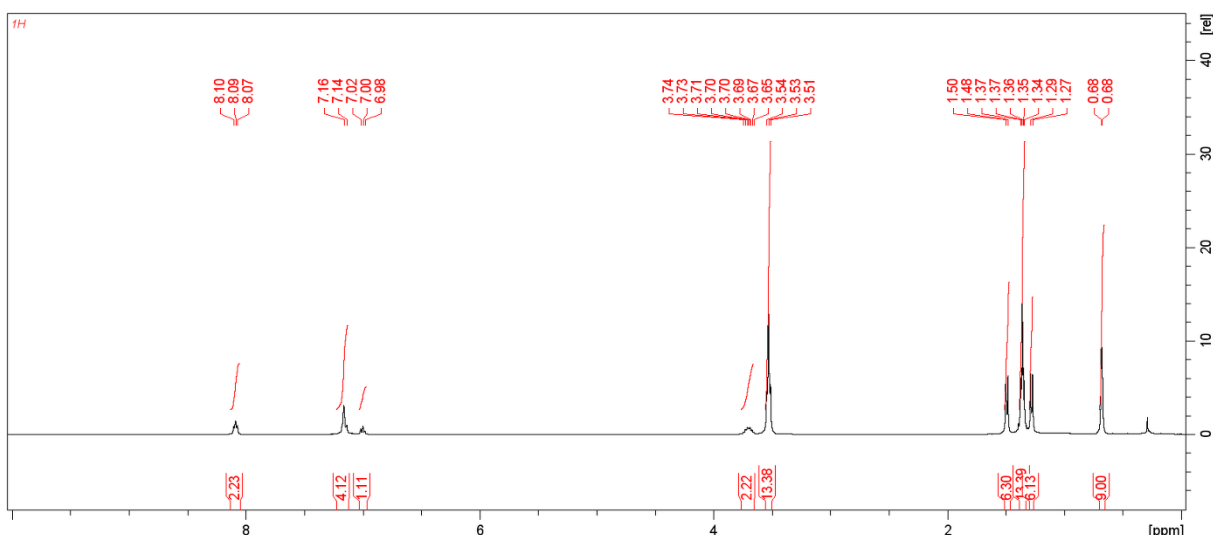


Figure S8. ¹H NMR (400 MHz, C₆D₆, 298 K) spectrum of isolated (*i*Pr₂N)PhP-P(SiMe₃)Li·3.3THF.

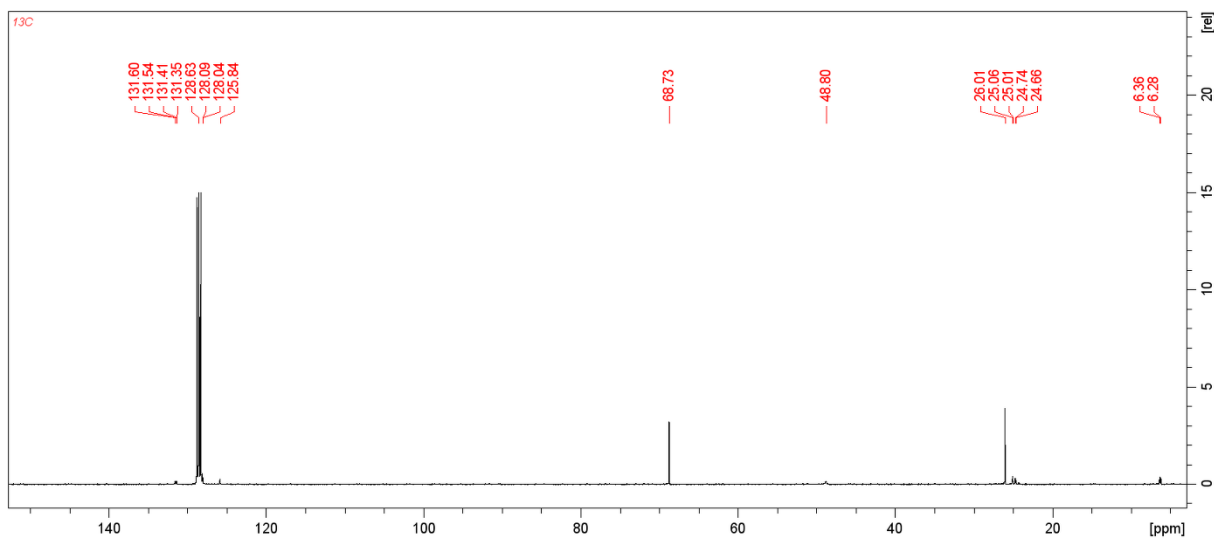


Figure S9. $^{13}\text{C}\{^1\text{H}\}$ NMR (100.6 MHz, C_6D_6 , 298 K) spectrum of isolated $(i\text{Pr}_2\text{N})\text{PhP-P}(\text{SiMe}_3)\text{Li}\cdot 3.3\text{THF}$.

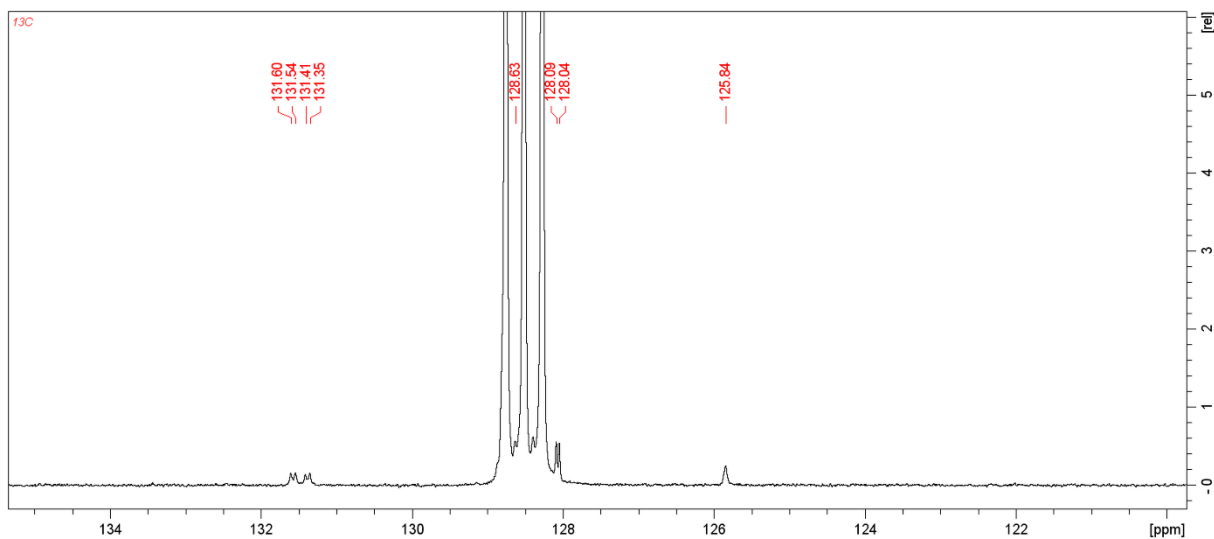


Figure S10. $^{13}\text{C}\{^1\text{H}\}$ NMR (100.6 MHz, C_6D_6 , 298 K) spectrum of isolated $(i\text{Pr}_2\text{N})\text{PhP-P}(\text{SiMe}_3)\text{Li}\cdot 3.3\text{THF}$ in the narrow range from 134 ppm to 120 ppm.

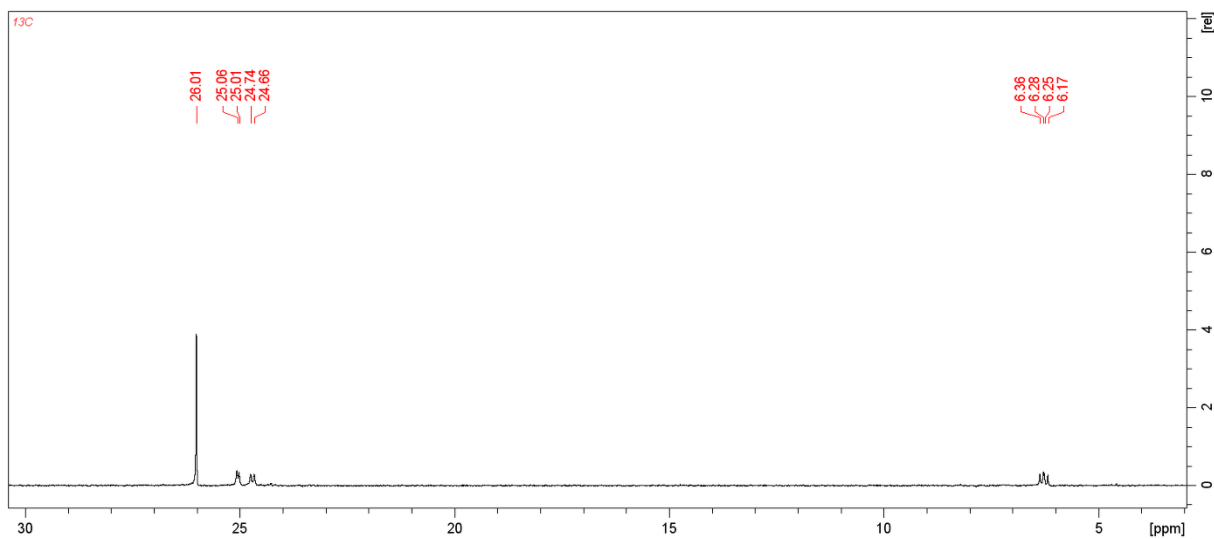


Figure S11. $^{13}\text{C}\{^1\text{H}\}$ NMR (100.6 MHz, C_6D_6 , 298 K) spectrum of isolated $(i\text{Pr}_2\text{N})\text{PhP-P}(\text{SiMe}_3)\text{Li}\cdot 3.3\text{THF}$ in the narrow range from 30 ppm to 0 ppm.

2.4. Ph₂C=P-PPh(NiPr₂) (3)

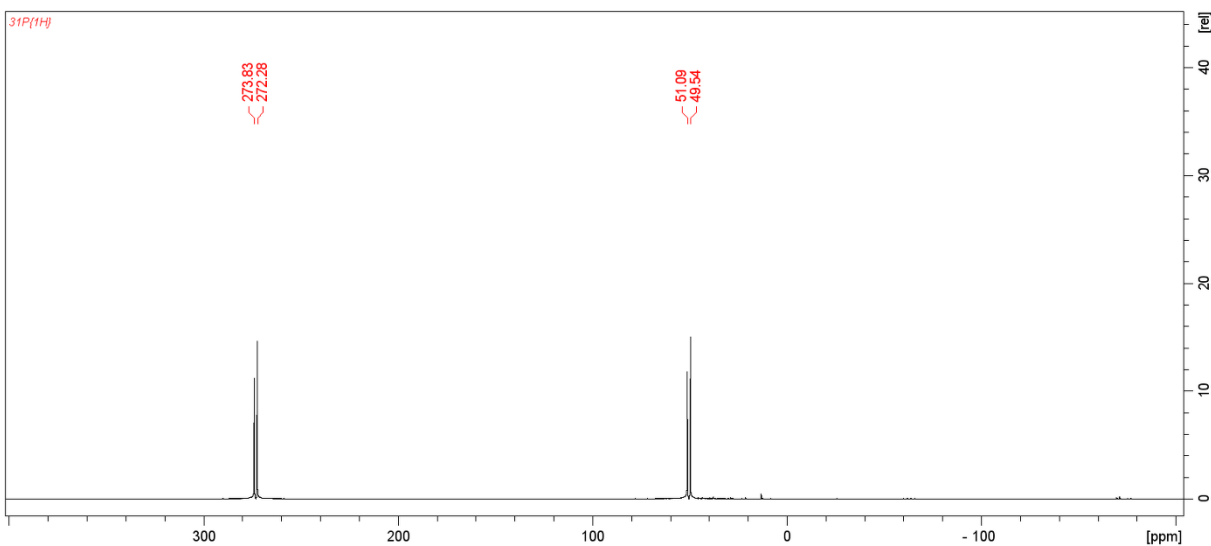


Figure S12. $^{31}\text{P}\{\text{H}\}$ NMR (162 MHz, Tol-d₈, 298 K) spectrum of isolated Ph₂C=P-PPh(NiPr₂).

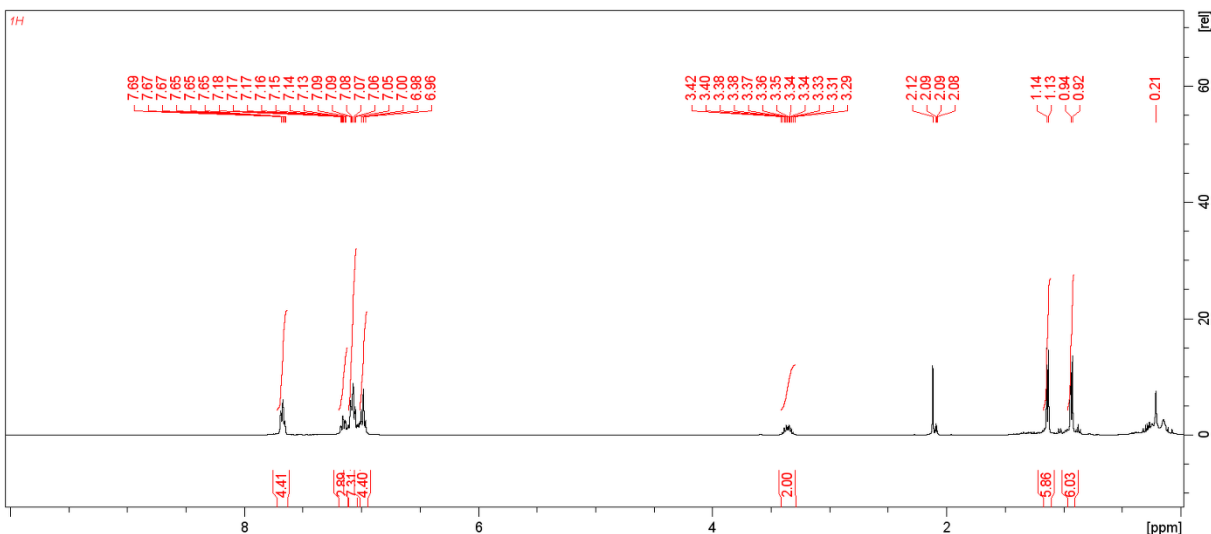


Figure S13. ^1H NMR (400 MHz, Tol-d₈, 298 K) spectrum of isolated Ph₂C=P-PPh(NiPr₂).

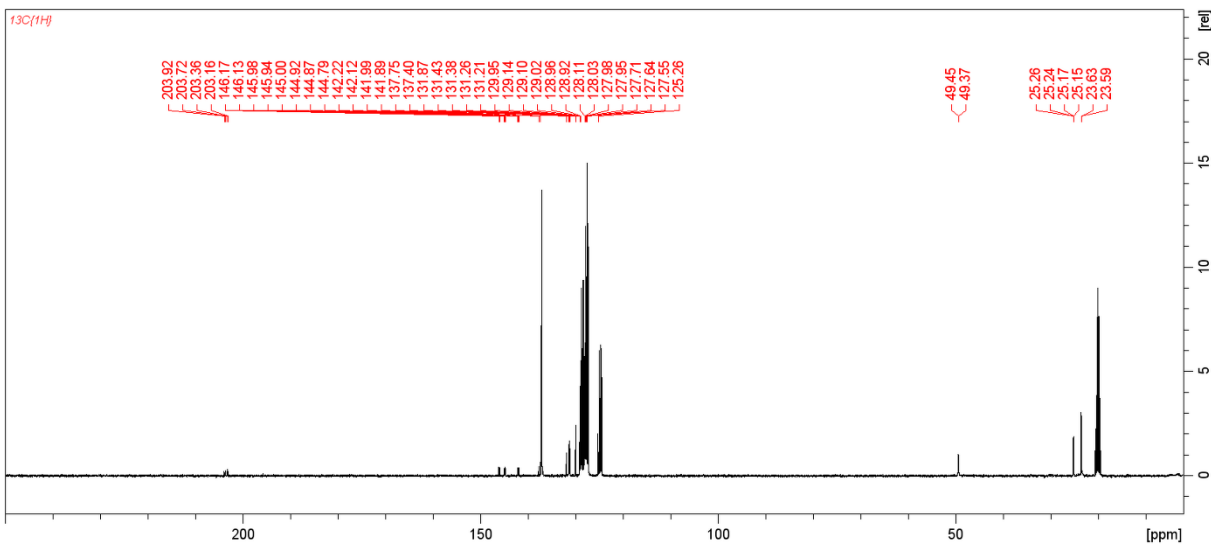


Figure S14. ¹³C{¹H} NMR (100.6 MHz, Tol-d₈, 298 K) spectrum of isolated Ph₂C=P-PPh(NiPr₂).

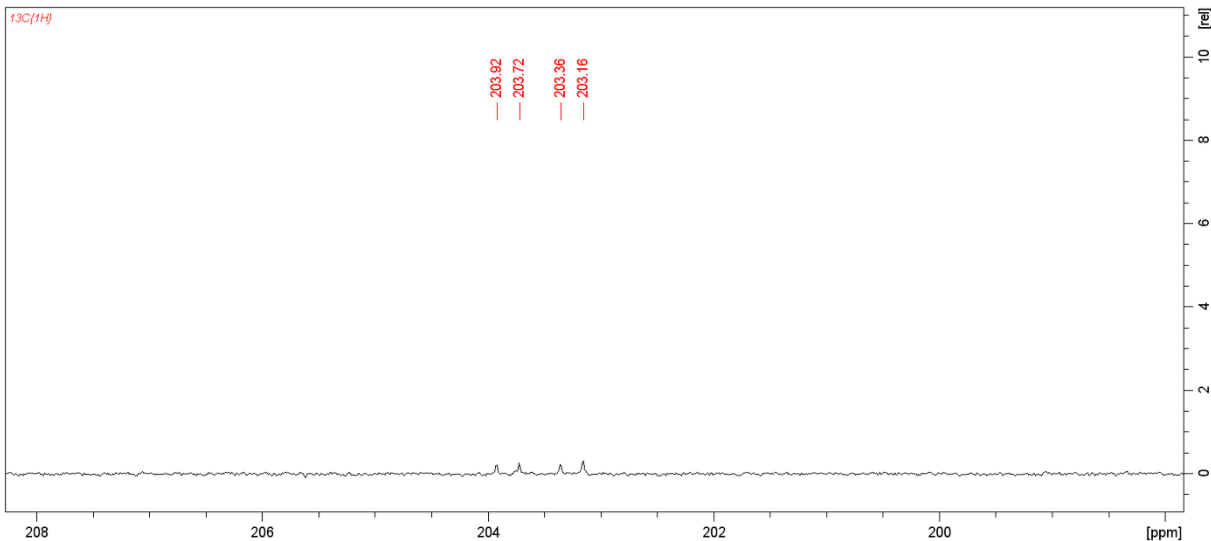


Figure S15. ¹³C{¹H} NMR (100.6 MHz, Tol-d₈, 298 K) spectrum of isolated Ph₂C=P-PPh(NiPr₂) in the narrow range from 208 ppm to 198 ppm.

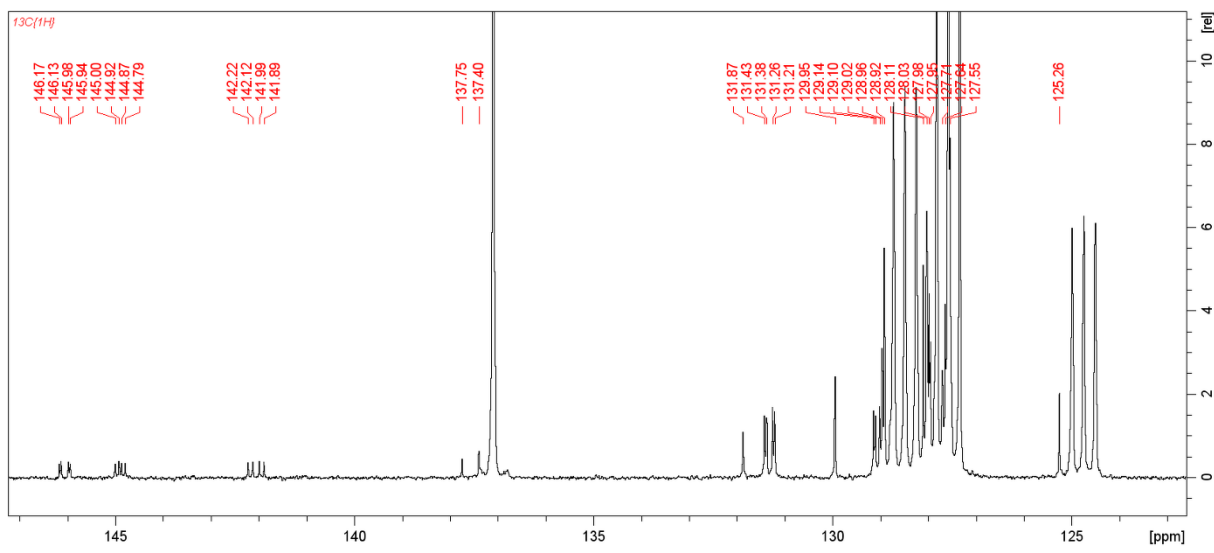


Figure S16. $^{13}\text{C}\{^1\text{H}\}$ NMR (100.6 MHz, Tol-d₈, 298 K) spectrum of isolated Ph₂C=P-PPh(NiPr₂) in the narrow range from 147 ppm to 123 ppm.

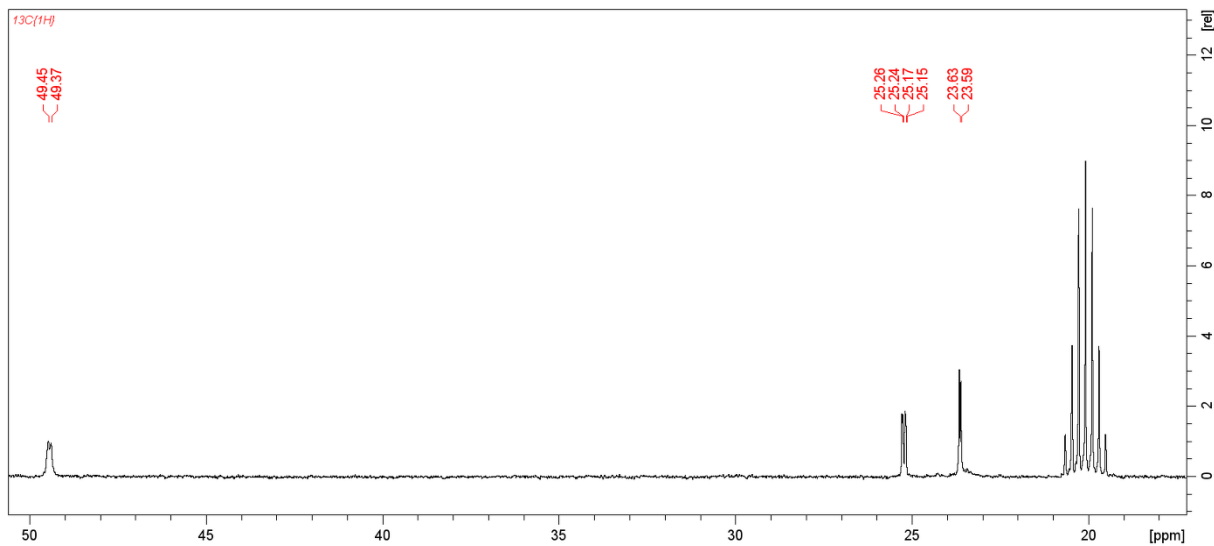


Figure S17. $^{13}\text{C}\{^1\text{H}\}$ NMR (100.6 MHz, Tol-d₈, 298 K) spectrum of isolated Ph₂C=P-PPh(NiPr₂) in the narrow range from 50 ppm to 18 ppm.

2.5. Reaction of Ph₂C=P-PPh(NiPr₂) with nBuLi

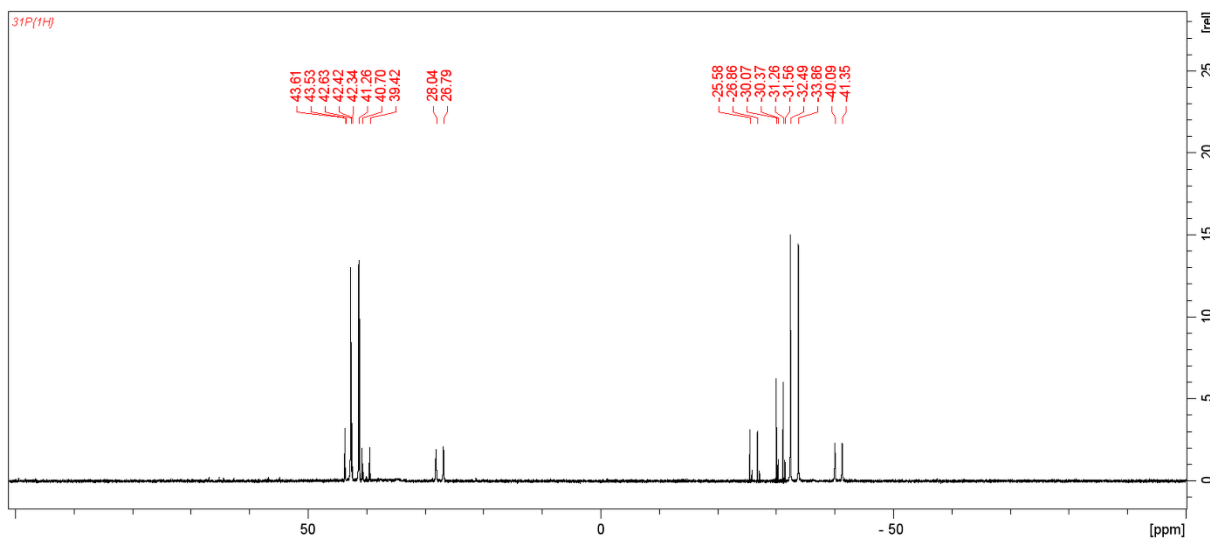


Figure S18. $^{31}\text{P}\{\text{H}\}$ NMR (162 MHz, THF-d₈, 298 K) spectrum measured from reaction mixture of Ph₂C=P-PPh(NiPr₂) with nBuLi.

- 43.02 ppm, d, $J_{\text{P-P}} = 192.5$ Hz, $[(i\text{Pr}_2\text{N})\text{PhP-P}(n\text{Bu})-\text{CPh}_2]\text{Li}$;
- 42.94 ppm, d, $J_{\text{P-P}} = 193.2$ Hz, $[(i\text{Pr}_2\text{N})\text{PhP-P}(n\text{Bu})-\text{CPh}_2]\text{Li}$;
- 41.94 ppm, d, $J_{\text{P-P}} = 223.0$ Hz, $[(i\text{Pr}_2\text{N})\text{PhP-P}(n\text{Bu})-\text{CPh}_2]^-, \text{Li}^+$;
- 40.06 ppm, d, $J_{\text{P-P}} = 208.3$ Hz, $[(i\text{Pr}_2\text{N})\text{PhP-P}(n\text{Bu})-\text{CPh}_2]^-\text{Li}$;
- 27.42 ppm, d, $J_{\text{P-P}} = 202.3$ Hz, $[(i\text{Pr}_2\text{N})\text{PhP-P}(n\text{Bu})-\text{CPh}_2]\text{Li}$;
- -26.22 ppm, d, $J_{\text{P-P}} = 208.3$ Hz, $[(i\text{Pr}_2\text{N})\text{PhP-P}(n\text{Bu})-\text{CPh}_2]\text{Li}$;
- -30.66 ppm, $J_{\text{P-P}} = 192.5$ Hz, $[(i\text{Pr}_2\text{N})\text{PhP-P}(n\text{Bu})-\text{CPh}_2]\text{Li}$;
- -30.97 ppm, $J_{\text{P-P}} = 193.2$ Hz, $[(i\text{Pr}_2\text{N})\text{PhP-P}(n\text{Bu})-\text{CPh}_2]\text{Li}$;
- -33.18 ppm, $J_{\text{P-P}} = 223.0$ Hz, $[(i\text{Pr}_2\text{N})\text{PhP-P}(n\text{Bu})-\text{CPh}_2]^-, \text{Li}^+$;
- -40.72 ppm, d, $J_{\text{P-P}} = 202.3$ Hz, $[(i\text{Pr}_2\text{N})\text{PhP-P}(n\text{Bu})-\text{CPh}_2]\text{Li}$;

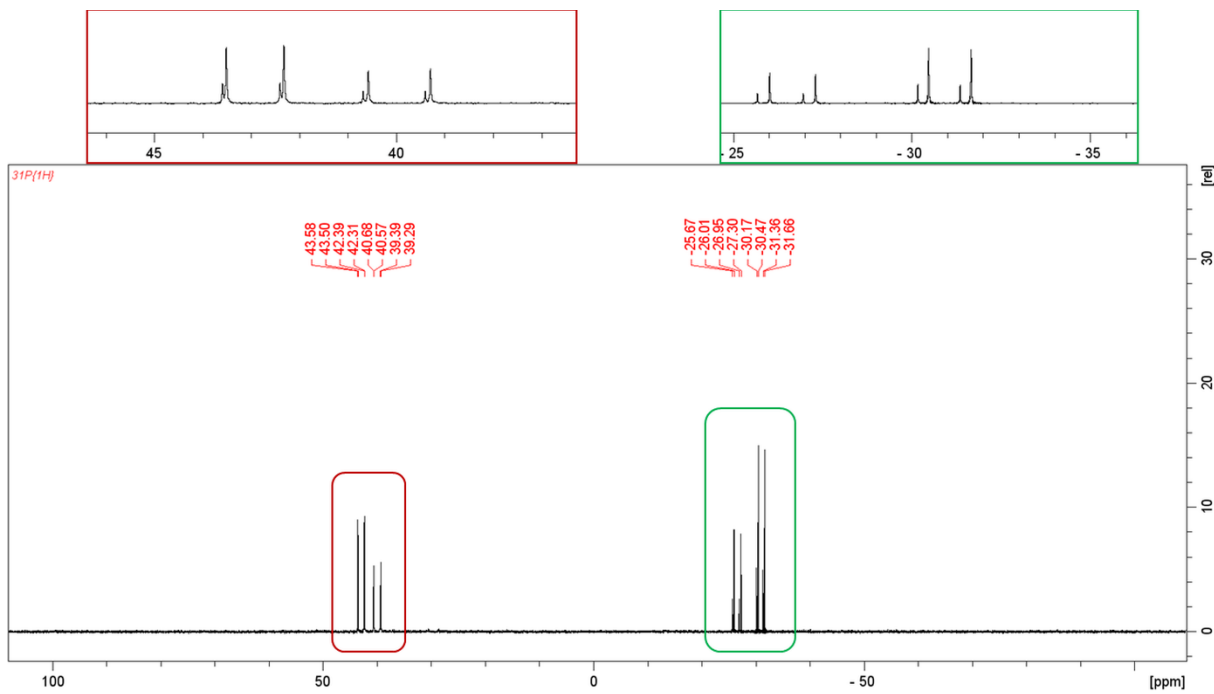


Figure S19. $^{31}\text{P}\{\text{H}\}$ NMR (162 MHz, THF-d₈, 298 K) spectrum measured from isolated crystals of $[(i\text{Pr}_2\text{N})\text{PhP-P}(n\text{Bu})-\text{CPh}_2]^-[\text{Li}(\text{DME})_3]^+$ (**3a**).

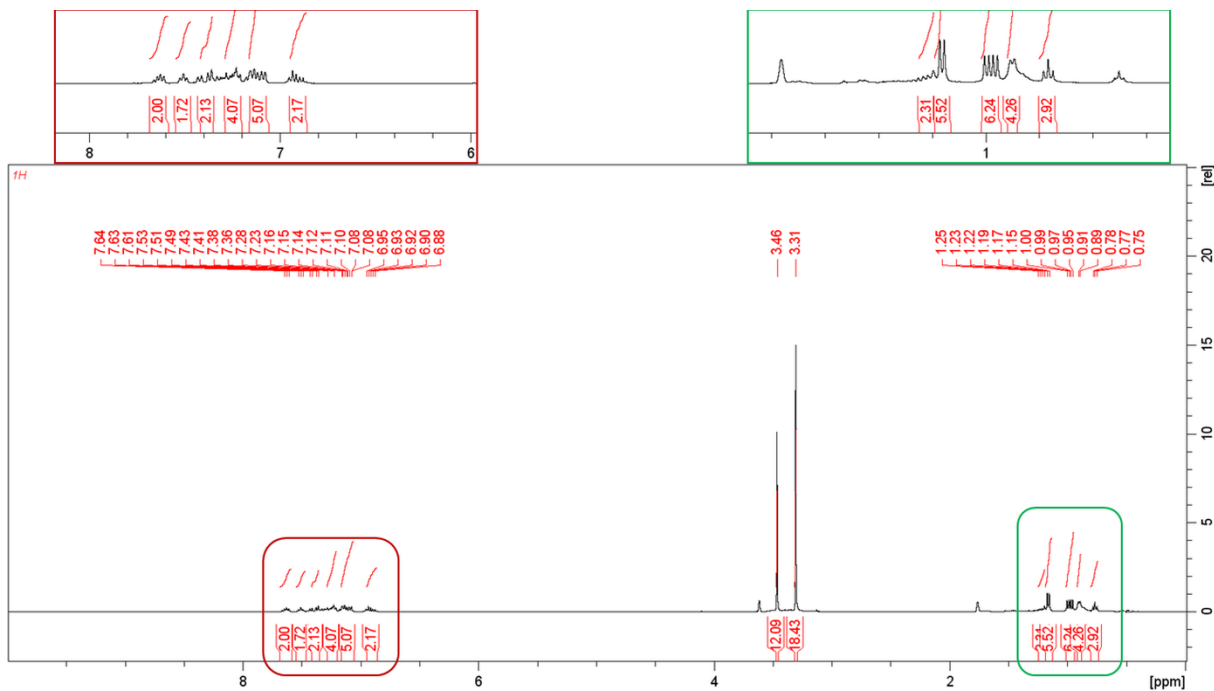


Figure S20. ^1H NMR (400 MHz, THF-d₈, 298 K) spectrum of isolated crystals of $[(i\text{Pr}_2\text{N})\text{PhP-P}(n\text{Bu})-\text{CPh}_2]^-[\text{Li}(\text{DME})_3]^+$.

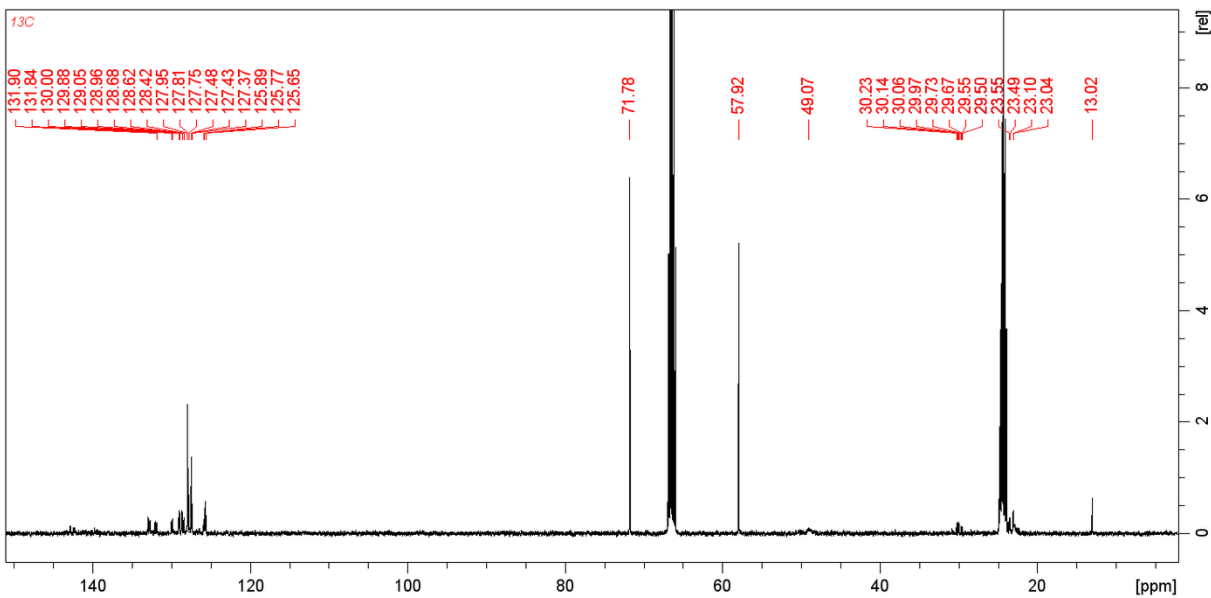


Figure S21. $^{13}\text{C}\{\text{H}\}$ NMR (100.6 MHz, THF-d₈, 298 K) spectrum of isolated crystals of $[(i\text{Pr}_2\text{N})\text{PhP}-\text{P}(n\text{Bu})-\text{CPh}_2]^-\text{[Li(DME)}_3]^+$.

2.6. Reaction of Ph₂C=P-PPh(NiPr₂) with PhLi

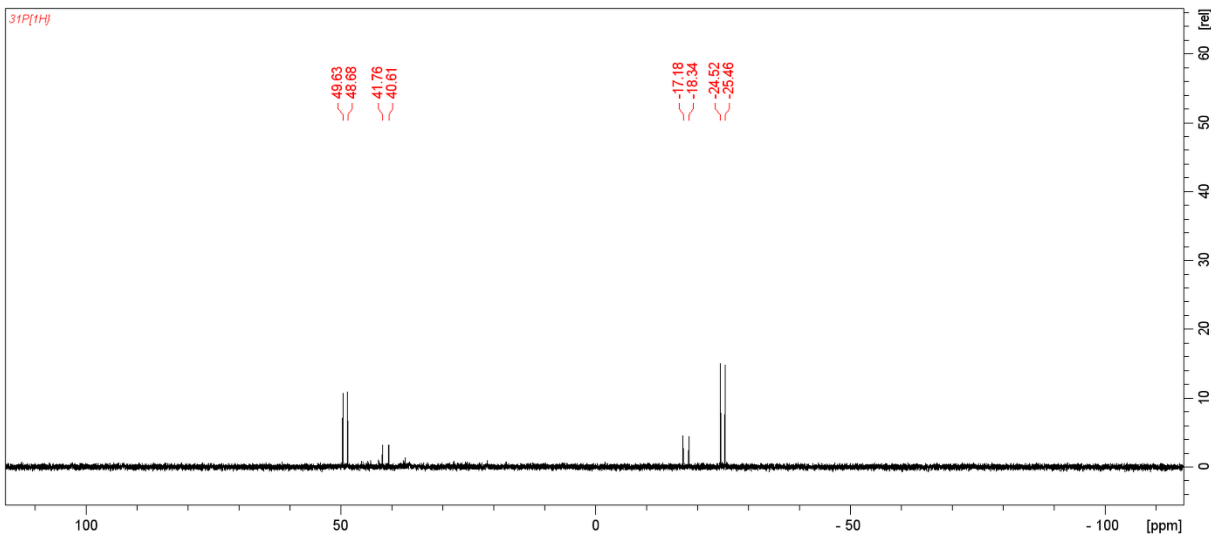


Figure S22. $^{31}\text{P}\{\text{H}\}$ NMR (162 MHz, THF-d₈, 298 K) spectrum measured from reaction mixture of Ph₂C=P-PPh(NiPr₂) with PhLi.

- 49.15 ppm, d, $J_{\text{P-P}} = 152.8$ Hz, $[(i\text{Pr}_2\text{N})\text{PhP-P(Ph)-CPh}_2]\text{Li}$;
- 41.18 ppm, d, $J_{\text{P-P}} = 186.5$ Hz, $[(i\text{Pr}_2\text{N})\text{PhP-P(Ph)-CPh}_2]\text{Li}$;
- -17.76 ppm, d, $J_{\text{P-P}} = 186.4$ Hz, $[(i\text{Pr}_2\text{N})\text{PhP-P(Ph)-CPh}_2]\text{Li}$;
- -24.99 ppm, d, $J_{\text{P-P}} = 152.8$ Hz, $[(i\text{Pr}_2\text{N})\text{PhP-P(Ph)-CPh}_2]\text{Li}$;

3. X-ray section

The X-ray diffraction data for **1**, **2** were measured with an STADIVARI diffractometer from STOE equipped with an EGER 1M CDTE detector and AXO Mo sources providing $\text{K}\alpha$ radiation by high-grade multilayer X-ray mirror optics for Mo ($\lambda = 0.71073 \text{ \AA}$) wavelengths. The measurements were carried out at 100 K (**1**) and at 273 K (**2**). The X-ray diffraction data for **1** was measured with an IPDS2T diffractometer equipped with an STOE image plate detector system and microfocus X-ray sources providing $\text{K}\alpha$ radiation by high-grade multilayer X-ray mirror optics for Mo ($\lambda = 0.71073 \text{ \AA}$). The measurements were carried out at 120 K. The structures were solved by direct methods and refined against F^2 with the Shelxs-2018 and Shelxl-2018 programs⁴ run under WinGX.⁵ Non-hydrogen atoms were refined with anisotropic displacement parameters. The isotropic displacement parameters of all hydrogens were fixed to 1.2 U_{eq} for aromatic, CH, CH_2 and 1.5 $U\text{K}_{\text{eq}}$ for methyl groups. For **5**, the contribution to the scattering of the disordered solvent molecule (THF) was removed with the SQUEEZE routine of the PLATON program.⁶

The crystallographic data for all structures reported in this paper have been deposited in the Cambridge Crystallographic Data Centre as supplementary publications No. CCDC 2432754-2432756. Copies of the data can be obtained free of charge upon application to the CCDC, 12 Union Road, Cambridge CB2 1EZ, UK (Fax: (+44) 1223-336-033; E mail: deposit@ccdc.cam.ac.uk).

3.1. Crystallographic data

Table S1. Crystallographic data for **1**, **2** and **3a**.

	(iPr ₂ N)PhP-P(SiMe ₃) ₂ (1)	(iPr ₂ N)PhP-P(SiMe ₃)Li · 3THF (2)	[(iPr ₂ N)PhP-P(<i>n</i> Bu)-CPh ₂] · [Li(DME) ₃] ⁺ (3a)
Empirical formula	C ₁₈ H ₃₇ NP ₂ Si ₂	C ₂₇ H ₅₂ LiNO ₃ P ₂ Si	C ₂₉ H ₃₈ NP ₂ ; C ₁₂ H ₃₀ LiO ₆
Formula weight	385.6	535.66	739.84
Radiation source	MoK\alpha	MoK\alpha	MoK\alpha
Wavelength [Å]	0.71073	0.71073	0.71073
Crystal System	monoclinic	monoclinic	triclinic
Space group	P2 ₁ /n	P2 ₁	P-1
<i>a</i> [Å]	10.4094(14)	16.6328(7)	11.1097(6)
<i>b</i> [Å]	12.1438(11)	18.6610(6)	11.8221(6)
<i>c</i> [Å]	18.347(3)	20.7350(10)	20.0269(10)
α [°]	90	90	102.679(4)
β [°]	93.115(11)	89.930(4)	94.734(4)
γ [°]	90	90	92.838(4)
<i>V</i> [Å ³]	2315.7(5)	6435.8(5)	2551.2(2)
<i>Z</i>	4	8	2
Calculated Density [g·cm ⁻¹]	1.106	1.106	0.963
T [K]	100(2)	273(2)	120(2)
μ [mm ⁻¹]	0.292	0.198	0.122
Theta range for data collection [°]	2.20 – 31.06	2.183 – 27	1.77 – 29.41
Index ranges	-14 ≤ <i>h</i> ≤ 14 -17 ≤ <i>k</i> ≤ 17 -26 ≤ <i>l</i> ≤ 25	-21 ≤ <i>h</i> ≤ 20 -23 ≤ <i>k</i> ≤ 23 -26 ≤ <i>l</i> ≤ 20	-12 ≤ <i>h</i> ≤ 14 -15 ≤ <i>k</i> ≤ 15 -25 ≤ <i>l</i> ≤ 25
Data / restraints / parameters	6527/0/218	19705/0.816/1214	11106/0/515
Goodness-of-fit on <i>F</i> ²	0.968	0.985	1.085
Final R indices	0.0626	0.0638	0.0939
[>2σ(<i>I</i>)]	0.1342	0.1448	0.1864
R indices (all data)	0.1414	0.0855	0.1614
[>2σ(<i>I</i>)] (all data)	0.1624	0.1567	0.2216
Largest diff. peak and hole [e.Å ⁻³]	0.099 and -0.422	0.077 and -0.35	0.061 and -0.367
CCDC	2432756	2432754	2432755

3.2. Molecular structures

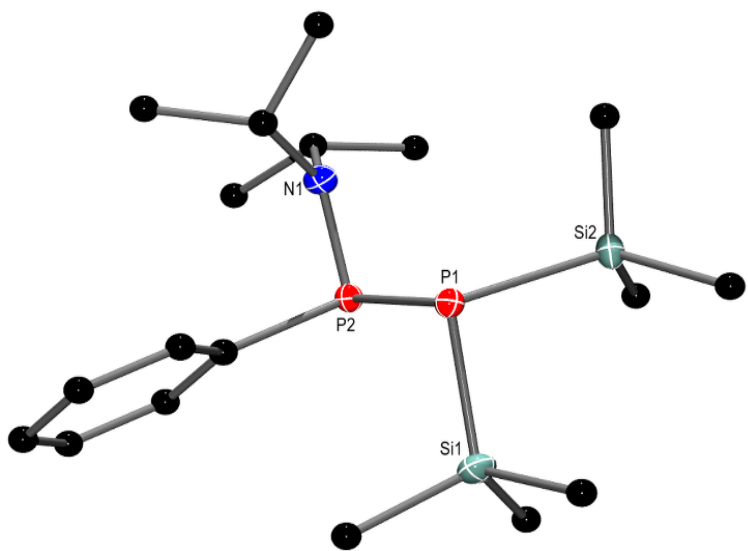


Figure S23. Molecular structure of $(i\text{Pr}_2\text{N})\text{PhP-P}(\text{SiMe}_3)_2$ (**1**) (ellipsoids 30%, the H atoms have been omitted for clarity). Important bond distances (Å) and angles (deg): P1–P2 2.2331(11), N1–P2 1.711(2), P1–Si1 2.2697(12), P1–Si2 2.2815(11); N1–P2–P1 102.52(9), P2–P1–Si1 99.96(4), P2–P1–Si2 100.33(4), Si1–P1–Si2 101.99(5).

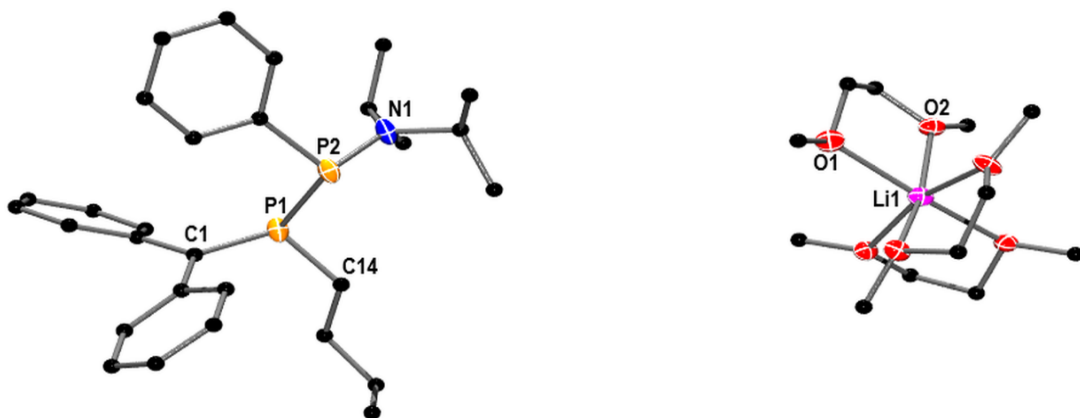


Figure S24. Molecular structure of ionic compound $[(i\text{Pr}_2\text{N})\text{PhP-P}(n\text{Bu})-\text{CPh}_2]^+[\text{Li}(\text{DME})_3]^+$ (**3a**) (ellipsoids 30%, the H atoms have been omitted for clarity). Important bond distances (Å) and angles (deg): P1–P2 2.2861(16), N1–P2 1.700(4), C1–P1 1.770(4), P1–C14 1.766(11), Li1–O1 2.044(10), Li1–O2 2.111(8); C1–P1–P2 111.33(14), C14–P1–P2 92.2(3), N1–P2–P1 102.89(14), O1–Li1–O2 77.3(3).

4. Theoretical Calculations

Table S2. Selected data from the DFT calculations (DFT-D3/def2-TZVP/BP86 and DFT-D3/b3-lyp/def2-TZVP).

Compound: Phosphanylphosphaalkene	Total energy	Dipole moment	HOMO-LUMO gap
	H	D	eV
Me ₂ C=P-PtBu ₂	-1116.5866	0.63	2.68
Me(Ph)C=P-PtBu ₂	-1308.38271	2.26	2.17
Ph ₂ C=P-PtBu ₂	-1500.19443	2.20	2.03
Me ₂ C=P-P(NEt ₂) ₂	-1227.34712	1.28	2.61
Me(Ph)C=P-P(NEt ₂) ₂	-1419.15658	1.28	2.33
Ph ₂ C=P-P(NEt ₂) ₂	-1610.97142	1.36	2.00
Ph ₂ C=P-PPh(NiPr ₂) (3)	-1941.73655	0.96	1.80

Table S3. Results of the Population Analysis Based On Occupation Numbers⁷ (DFT-D3/def2-TZVP/BP86 and DFT-D3/b3-lyp/def2-TZVP).

Compound	Two center shared electron numbers					Atomic charges with multicenter corrections					
	N ¹ -P ¹	N ² -P ¹	N-P _{avg.}	P-P	P-C	N ¹	N ²	N _{avg.}	P ¹	P ²	C
Me ₂ C=P-PtBu ₂				1.12	1.89				0.07	-0.08	-0.03
Me(Ph)C=P-PtBu ₂				1.13	1.84				0.09	-0.08	-0.03
Ph ₂ C=P-PtBu ₂				1.17	1.77				0.13	-0.04	-0.07
Me ₂ C=P-P(NEt ₂) ₂	1.13	1.15	1.14	1.09	1.89	-0.18	-0.18	-0.18	0.28	-0.11	-0.04
Me(Ph)C=P-P(NEt ₂) ₂	1.16	1.13	1.15	1.08	1.87	-0.17	-0.17	-0.17	0.28	-0.10	-0.03
Ph ₂ C=P-P(NEt ₂) ₂	1.15	1.13	1.14	1.08	1.80	-0.18	-0.17	-0.17	0.29	-0.11	-0.03
Ph ₂ C=P-PPh(NiPr ₂) (3)	1.23			1.05	1.81	-0.13			0.23	-0.13	0.00

Table S4. Wiberg bond indices⁸ (DFT-D3/def2-TZVP/BP86 and DFT-D3/b3-lyp/def2-TZVP).

Compound	Wiberg bond index				
	N ¹ -P	N ² -P	N-P _{avg.}	P-P	P-C
Me ₂ C=P-PtBu ₂				1.06	1.77
Me(Ph)C=P-PtBu ₂				1.10	1.69
Ph ₂ C=P-PtBu ₂				1.17	1.59
Me ₂ C=P-P(NEt ₂) ₂	1.09	0.97	1.03	1.06	1.70
Me(Ph)C=P-P(NEt ₂) ₂	1.10	1.12	1.11	1.05	1.76
Ph ₂ C=P-P(NEt ₂) ₂	1.08	1.10	1.09	1.04	1.67
Ph ₂ C=P-PPh(NiPr ₂) (3)	1.07			1.03	1.68

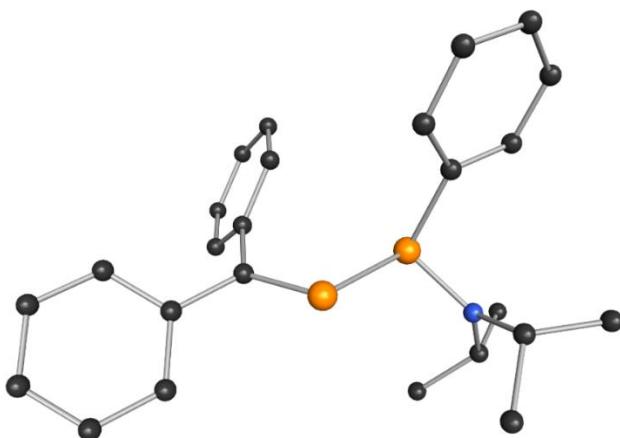


Figure S25. Molecular structures of **3** (hydrogen atoms omitted for clarity, DFT-D3: b3-lyp; def2-TZVP).

Below are presented xyz coordinates for optimized geometry of **3**:

```

C -1.3628811 -0.4817154 -1.6453855
C -1.0902435 -1.9121036 -1.3889609
C 0.2000997 -2.4479890 -1.4642482
H 1.0220579 -1.8152120 -1.7695883
C 0.4331851 -3.7890944 -1.1840696
H 1.4397822 -4.1821071 -1.2544116
C -0.6176338 -4.6187588 -0.8132806
H -0.4355662 -5.6621916 -0.5880380
C -1.9091584 -4.1015837 -0.7400174
H -2.7343322 -4.7412508 -0.4518678
C -2.1452819 -2.7682844 -1.0388042
H -3.1516000 -2.3725357 -0.9869696
C -2.4720297 -0.1831988 -2.5825584
C -2.6591576 -0.9779028 -3.7249488
H -1.9981504 -1.8168184 -3.8994633
C -3.6645494 -0.6918103 -4.6371340
H -3.7819092 -1.3120717 -5.5172695
C -4.5192043 0.3858501 -4.4240523
H -5.3090666 0.6038725 -5.1320291
C -4.3588530 1.1731375 -3.2882640
H -5.0301146 2.0028739 -3.1038316
C -3.3493140 0.8922229 -2.3778755
H -3.2441100 1.4939486 -1.4846499
C 2.4097804 -0.0006374 0.1629841
C 3.3965915 -0.2625919 1.1228636
H 3.1044322 -0.4421321 2.1508050
C 4.7399124 -0.2949647 0.7767126
H 5.4859986 -0.4968001 1.5358920
C 5.1284489 -0.0773255 -0.5434284
H 6.1763216 -0.1050244 -0.8151883

```

```

C  4.1611572  0.1777325 -1.5070344
H  4.4517234  0.3564805 -2.5352485
C  2.8142830  0.2198998 -1.1554210
H  2.0770378  0.4410061 -1.9181658
C  -0.1912919  0.9471625  3.1100611
H  -0.1326723  1.8825948  3.6692073
C  -1.6742743  0.6832889  2.8261108
H  -2.2399085  0.6276420  3.7595498
H  -1.8065299  -0.2622015  2.2956317
C  0.4151728  -0.1453285  3.9954743
H  -0.1414826  -0.2347911  4.9315361
H  0.3868179  -1.1128407  3.4904587
C  1.1576472  2.5103541  1.6521037
H  1.6535016  2.4654712  0.6806350
C  0.0815572  3.5998766  1.5671012
H  -0.4451176  3.7220198  2.5161667
H  0.5399322  4.5605096  1.3206342
C  2.2314122  2.8617312  2.6881451
H  1.8145009  2.9148089  3.6965171
H  2.6715321  3.8357093  2.4625864
N  0.5979718  1.1636374  1.8780698
P  0.6543220  -0.0895261  0.7270080
P  -0.5146429  0.8334095  -0.9667987
H  -2.0962075  1.4793451  2.2109760
H  1.4546284  0.0874586  4.2328557
H  -0.6504851  3.3609626  0.7957810
H  3.0259604  2.1157858  2.6831363

```

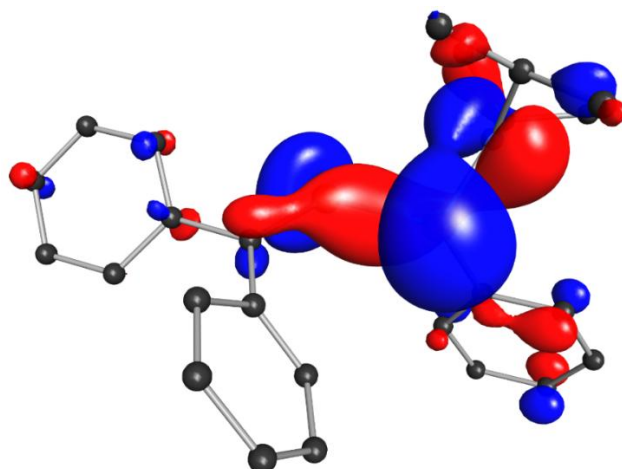


Figure S26. HOMO of **3** (hydrogen atoms omitted for clarity, DFT-D3: b3-lyp; def2-TZVP, isosurface 0.04).

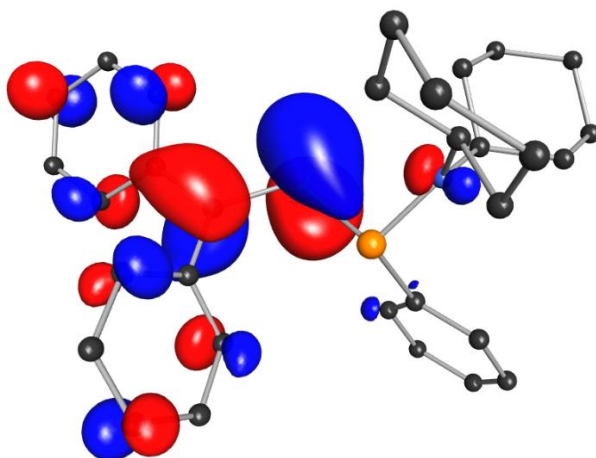


Figure S27. LUMO of **3** (hydrogen atoms omitted for clarity, DFT-D3: b3-lyp; def2-TZVP, isosurface 0.04).

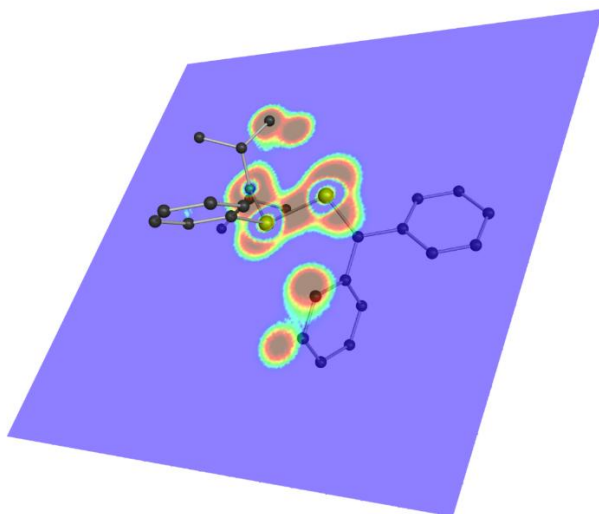


Figure S28. Electron localization function of **3** projection onto the P1P2N plane (hydrogen atoms omitted for clarity, DFT-D3: b3-lyp; def2-TZVP, isoplot 0.2 to 0.8).

DFT quantum chemical calculations were performed using Turbomole 7.7.1 software package.^{9, 10} Molecular geometries were optimized using the resolution-of-the-identity¹¹⁻¹⁴ approximation and multiple accelerated resolution of identity¹⁵ approximation. Basis sets def2-TZVP¹⁶ together with b3-lyp^{17, 18} functional were used. D3 dispersion correction was applied.¹⁹ Energetic minima were confirmed by analytical calculations of vibrations with aoforce²⁰ module. Graphics were generated with BIOVIA Tmolex 2024 software.²¹

5. References

1. N. Szynkiewicz, L. Ponikiewski and R. Grubba, *Dalton Trans.*, 2018, **47**, 16885-16894.
2. A. H. Cowley, M. J. S. Dewar, W. R. Jackson, Jr. and W. B. Jennings, *J. Am. Chem. Soc.*, 1970, **92**, 5206-5213.
3. G. Fritz and W. Hölderich, *Z. anorg. allg. Chem.*, 1976, **422**, 104-114.
4. G. Sheldrick, *Acta Crystallogr. C*, 2015, **71**, 3-8.
5. L. Farrugia, *J. Appl. Cryst.*, 2012, **45**, 849-854.
6. A. Spek, *Acta Crystallogr. C* 2015, **71**, 9-18.
7. C. Ehrhardt and R. Ahlrichs, *Theor. Chim. Acta*, 1985, **68**, 231-245.
8. K. B. Wiberg, *Tetrahedron*, 1968, **24**, 1083-1096.
9. O. Treutler and R. Ahlrichs, *J. Chem. Phys.*, 1995, **102**, 346-354.
10. M. Von Arnim and R. Ahlrichs, *J. Comput. Chem.*, 1998, **19**, 1746-1757.
11. K. Eichkorn, O. Treutler, H. Öhm, M. Häser and R. Ahlrichs, *Chem. Phys. Lett.*, 1995, **240**, 283-290.
12. K. Eichkorn, O. Treutler, H. Öhm, M. Häser and R. Ahlrichs, *Chem. Phys. Lett.*, 1995, **242**, 652-660.
13. K. Eichkorn, F. Weigend, O. Treutler and R. Ahlrichs, *Theor. Chem. Acc.*, 1997, **97**, 119-124.
14. F. Weigend, *Phys. Chem. Chem. Phys.*, 2006, **8**, 1057-1065.
15. M. Sierka, A. Hogekamp and R. Ahlrichs, *J. Chem. Phys.*, 2003, **118**, 9136-9148.
16. F. Weigend and R. Ahlrichs, *Phys. Chem. Chem. Phys.*, 2005, **7**, 3297-3305.
17. A. D. Becke, *J. Chem. Phys.*, 1993, **98**, 5648-5652.
18. C. Lee, W. Yang and R. G. Parr, *Phys. Rev. B*, 1988, **37**, 785-789.
19. S. Grimme, J. Antony, S. Ehrlich and H. Krieg, *J. Chem. Phys.*, 2010, **132**.
20. P. Deglmann, F. Furche and R. Ahlrichs, *Chem. Phys. Lett.*, 2002, **362**, 511-518.
21. C. Steffen, K. Thomas, U. Huniar, A. Hellweg, O. Rubner and A. Schroer, *J. Comput. Chem.*, 2010, **31**, 2967-2970.